

## THE X-RAY LIGHT CURVE OF $\eta$ CARINAE: REFINEMENT OF THE ORBIT AND EVIDENCE FOR PHASE-DEPENDENT MASS LOSS

M. F. CORCORAN,<sup>1,2</sup> K. ISHIBASHI,<sup>3</sup> J. H. SWANK,<sup>2</sup> AND R. PETRE<sup>2</sup>

Received 2000 June 16; accepted 2000 September 24

### ABSTRACT

We solve the *Rossi X-Ray Timing Explorer* X-ray light curve of the extremely luminous and massive star  $\eta$  Carinae with a colliding-wind emission model to refine the ground-based orbital elements. The sharp decline to X-ray minimum at the end of 1997 fixes the date of the last periastron passage at  $1997.95 \pm 0.05$ , not 1998.13 as derived from ground-based radial velocities. This helps resolve a discrepancy between the ground-based radial velocities and spatially resolved velocity measures obtained by Space Telescope Imaging Spectrograph (STIS). The X-ray data are consistent with a mass function  $f(M) \approx 1.5$ , lower than the value  $f(M) \approx 7.5$  previously reported, so that the masses of  $\eta$  Carinae and the companion are  $M_\eta \geq 80 M_\odot$  and  $M_c \sim 30 M_\odot$ , respectively. In addition, the X-ray data suggest that the mass-loss rate from  $\eta$  Carinae is generally less than  $3 \times 10^{-4} M_\odot \text{ yr}^{-1}$ , about a factor of 5 lower than that derived from some observations in other wave bands. We could not match the duration of the X-ray minimum with any standard colliding-wind model in which the wind is spherically symmetric and the mass-loss rate is constant. However, we show that we can match the variations around X-ray minimum if we include an increase of a factor of  $\sim 20$  in the mass-loss rate from  $\eta$  Carinae for approximately 80 days following periastron. If real, this excess in  $\dot{M}$  would be the first evidence of enhanced mass flow off the primary when the two stars are close (presumably driven by tidal interactions). Our interpretation of the X-ray data suggests that the *ASCA* and *RXTE* X-ray spectra near the X-ray minimum are significantly contaminated by unresolved hard emission ( $E \geq 2$  keV) from some other nearby source, probably associated with scattering of the colliding-wind emission by circumstellar dust. Based on the X-ray fluxes, the distance to  $\eta$  Carinae is 2300 pc with formal uncertainties of only  $\sim 10\%$ .

*Subject headings:* binaries: general — stars: individual ( $\eta$  Carinae) — stars: variables: other — X-rays: stars

### 1. INTRODUCTION

Discovery of cyclical variations in the strength of the He I  $\lambda 10830$  line (Damineli 1996), the X-ray flux (Corcoran et al. 1995; Ishibashi et al. 1999), and radio emission (Duncan et al. 1995) spurred the suggestion that the supermassive star  $\eta$  Carinae is, in fact, a binary system (Damineli 1996; Damineli, Conti, & Lopes 1997; Corcoran et al. 1997) in which the variable phenomena over all wavelengths are driven by wind-wind interactions. Since the formation and evolution of massive binaries proceed via mechanisms distinct from those available to single stars (Vanbeveren, De Loore, & Van Rensbergen 1998), the presence of a companion would have a profound impact on our understanding of the formation and evolution of  $\eta$  Carinae, in particular, and of extremely massive stars, in general, and it is essential that we resolve this issue one way or another.

However, the “binary model” as proposed faces three major observational difficulties. The first concerns the variation of the X-ray emission from the source as measured by the *Rossi X-Ray Timing Explorer* (*RXTE*; Bradt, Rothschild, & Swank 1993). First attempts to model the observed *RXTE* 2–10 keV X-ray variability (Ishibashi et al. 1999) showed qualitative similarities to the observed variations in flux and column density but could not describe the X-ray variability near the X-ray minimum if the orbital elements

derived from ground-based radial velocity data (Damineli et al. 1997; Davidson 1997) were assumed. A second problem is that the column density to the X-ray source as measured by the *ASCA* satellite (Tanaka, Inoue, & Holt 1994) is lower, not higher, than the value outside eclipse, and no increase in flux was seen to energies of 10 keV, in contrast to model predictions (Corcoran et al. 2000). Finally, expected radial velocity variations (Damineli, Lopes, & Conti 1999) were not confirmed by subsequent *HST*/Space Telescope Imaging Spectrograph (STIS) observations of the stellar emission resolved from contamination by nearby circumstellar emission (Davidson et al. 2000). A more recent solution of the ground-based data (Damineli et al. 2000) does better to reconcile the velocity curve with the STIS measurements but does not adequately resolve the problems with the observed X-ray variations. Since the only observable spectral features are emission lines, there is the real possibility that the variation of the emitting gas may not faithfully represent the motion of the star, which means that deriving a true stellar radial velocity curve from the emission-line analysis alone may be difficult no matter what spatial resolution is available.

A more recent analysis of the *RXTE* data by Ishibashi (1999) showed that the match between the model and the X-ray light curve could be improved if the orbital elements were relaxed from the ground-based values. Here we try to use the X-ray light curve to attempt to refine the orbit. We find that we can generate an improved match to the *RXTE* fluxes if the time of periastron passage is earlier, the eccentricity higher, and the mass function lower than given in the Damineli et al. (2000) orbital solution. Most importantly, we find that the width of the X-ray minimum requires a

<sup>1</sup> Universities Space Research Association, 7501 Forbes Boulevard, Suite 206, Seabrook, MD 20706.

<sup>2</sup> Laboratory for High Energy Astrophysics, Goddard Space Flight Center, Greenbelt, MD 20771.

<sup>3</sup> National Research Council, Laboratory for Astronomy and Space Physics, Goddard Space Flight Center, Greenbelt, MD 20771.

suppression of the observed flux for an extended period following periastron. One way to do this is to increase the mass-loss rate from  $\eta$  Carinae by a factor of 20 for a brief period just after periastron passage. In the rest of the paper, we describe our analysis of the X-ray light curve. In § 2 we discuss the data extraction. In § 3 we describe the colliding-wind model and discuss our attempts to solve the X-ray light curve, and in § 4 we present our conclusions.

## 2. OBSERVATIONS AND DATA REDUCTION

We use data obtained by the *RXTE* proportional counter array (PCA). Data extraction and instrumental background correction are as described in Ishibashi et al. (1999). Most of the early data were obtained using 3 proportional counter units (PCUs), though we also include scaled 2 PCU mode data in the light curve, since most of the data available after 1998 is in 2 PCU mode. To convert these rates to flux, we use a linear conversion derived by comparison of *RXTE* and spatially resolved X-ray fluxes measured by contemporaneous observations of  $\eta$  Carinae with the *ASCA* X-ray satellite. There are four *ASCA* observations which overlap *RXTE* pointings within 2 days or less. We derived source fluxes from the *ASCA* data by direct fitting of the extracted spectrum, corrected for instrumental background and for sky background (where “sky” is the region beyond the 3' radius circle used to extract the *ASCA* source spectrum), as described in Corcoran et al. (1998, 2000). We then compared these fluxes to the *RXTE* count rate corrected for instrumental background. Figure 1 shows the *ASCA* fluxes and the *RXTE* net rates. A fit to these data yields  $f_x = 0.26(N - 7.66)$ , where  $f_x$  is the 2–10 keV flux seen by *RXTE* (in units of  $10^{-11}$  ergs  $\text{cm}^{-2}$   $\text{s}^{-1}$ ), and  $N$  is the *RXTE* 3 PCU rate corrected for instrumental background. Thus the sky background contributes about 7.66 counts  $\text{s}^{-1}$  to every 3 PCU observation. This value is slightly lower than the value used in Ishibashi et al. (1999) by about 1 count  $\text{s}^{-1}$  per 3 PCUs.

We also included *RXTE* “quicklook” data for the period since mid-1998. For each observation, we extracted PCA rates for the intervals when the satellite was on target; we then corrected these data for instrumental background in the same manner as used for the processed data. Since many

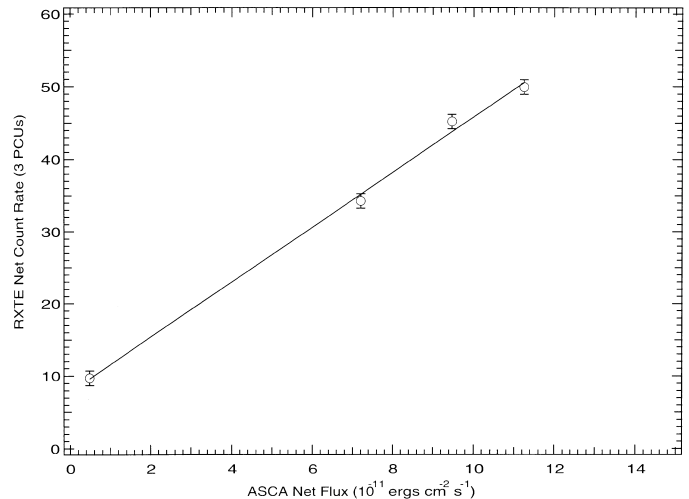


FIG. 1.—Plot of *RXTE* count rates vs. contemporaneous *ASCA* 2–10 keV source flux. The *RXTE* rates have been corrected for instrumental background. The straight line shows the best fit to the data.

of these data were obtained in 2 PCU mode, we performed an additional scaling to correct the 2 PCU data to approximate 3 PCU rates. We compared these net rates to the *RXTE* fluxes derived from the processed data in the intervals of overlap. We found that the scaling from the corrected quicklook net rates to observed 2–10 keV flux is  $f_x = 0.29(N_{\text{ql}} - 8.86)$ , where  $f_x$  is the 2–10 keV flux (in units of  $10^{-11}$  ergs  $\text{cm}^{-2}$   $\text{s}^{-1}$ ) and  $N_{\text{ql}}$  the corrected quicklook rates.

Figure 2 shows the *RXTE* light curve in the interval 1996 February through 2000 March. This light curve includes the data published in Ishibashi et al. (1999) and more recent observations. For our purposes, the significant characteristics are these: (1) a gradual increase in count rate starting at 1997.0; (2) a rapid rise to maximum and even faster decline to minimum at the end of 1997; (3) a gradual brightening of the X-ray flux coming out of the X-ray minimum; and (4) asymmetric maxima just prior to and just after the X-ray eclipse. Also apparent in the light curve are higher frequency “flares” (Corcoran et al. 1997; Ishibashi et al.

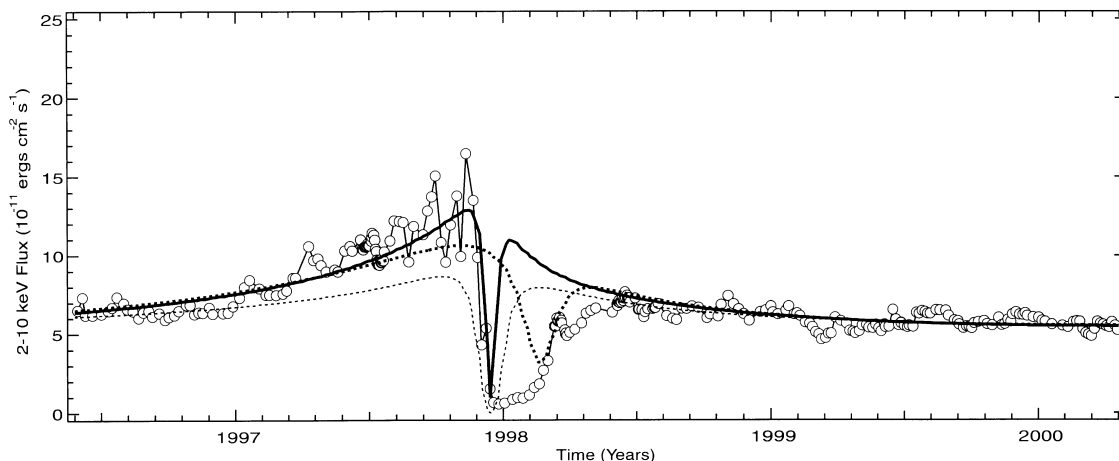


FIG. 2.—*RXTE* light curve of  $\eta$  Carinae and the colliding-wind model (thick solid line). The thick dotted line is the model derived using the orbital elements in Damiani et al. (2000), with  $f(m) = 7.5$ . The model based on the Damiani et al. (2000) parameters does not fit the abrupt decline in the observed 2–10 keV X-ray flux. Neither model fits the width of the X-ray eclipse adequately. The thin dotted line shows the effect of increasing  $\dot{M}_\eta$  to  $3 \times 10^{-4} M_\odot \text{yr}^{-1}$ .

1999); in what follows we make no attempt to try to explain or fit these higher frequency variations.

### 3. X-RAY LIGHT-CURVE ANALYSIS

The colliding-wind emission model we use is based on the Usov (1992) model used in Ishibashi et al. (1999). We fix the period of the binary orbit at 5.52 years (Damineli 1996), since this value seems to describe the He I  $\lambda 10830$  variations (Damineli 1996), the radio variability (Duncan et al. 1995), and the recurrent X-ray low state (Ishibashi et al. 1999). We take the orbital elements as given in Damineli et al. (2000) as a starting point, and, since the variations in He I  $\lambda 10830$  and the radio emission suggest an eclipse of a source of UV radiation presumably provided by the companion (Damineli et al. 1997; Duncan et al. 1995), we consider solutions in which the companion is a strong UV source, which restricts the mass of the companion to  $M_c > 15 M_\odot$ . We further assume that the winds collide at terminal velocities and take  $V_{\infty,\eta} = 500 \text{ km s}^{-1}$  (Hillier et al. 2000) and  $V_{\infty,c} = 2000 \text{ km s}^{-1}$  as reasonable values for the terminal velocities of  $\eta$  Carinae and the companion, respectively.

#### 3.1. A Constant- $\dot{M}$ Model

Table 1 lists the orbital elements we used to derive the model curves presented in Figures 2 and 3. After some experimenting, we adopted mass-loss rates  $\dot{M}_\eta = 1 \times 10^{-4}$

$M_\odot \text{ yr}^{-1}$  for  $\eta$  Carinae and  $\dot{M}_c = 1 \times 10^{-5} M_\odot \text{ yr}^{-1}$  for the companion. We adopted  $80 M_\odot$  as the mass for  $\eta$  Carinae and found that a companion mass  $M_c \sim 30 M_\odot$  provided a suitable fit to both the X-ray light curve and the STIS radial velocities. These component masses are similar to those described by Davidson (1999). However, our analysis is not very sensitive to the values of the component masses, and we find that we can fit the X-ray and STIS data with larger values of  $\eta$  Carinae's mass, or smaller component masses, or some combination. We allowed the eccentricity  $e$ , time of periastron passage  $T_0$ , and the terminal velocity of the wind of  $\eta$  Carinae  $V_{\infty,\eta}$  to vary to improve the fit to the *RXTE* light curve. We found that in order to match the rapid drop in X-ray brightness, the value of  $\omega$  needed to be near  $270^\circ$  with periastron passage  $T_0 = 1997.95$ , with an estimated uncertainty in  $T_0$  of  $\pm 0.05$  years. These parameters ensure that the line of sight at periastron passes through the thickest part of the wind from  $\eta$  Carinae if  $i < 60^\circ$ . While our adopted value of  $\omega$  is the same as that of Damineli et al. (2000), the sharp decline to minimum in the X-ray data fixes periastron passage to occur about 73 days earlier than the Damineli et al. (2000) value. We also derive an eccentricity  $e = 0.9$ , which is higher than the highest previously published value,  $e = 0.8$  (Davidson 1999). The smooth solid curve in Figure 2 is the colliding-wind emission based on our adopted parameters; the model

TABLE 1  
COLLIDING-WIND MODEL PARAMETERS

Parameter	Present Work	Damineli et al. 2000 Value
$T_0$ (periastron) .....	$1997.95 \pm 0.05$	1998.13
$e$ .....	0.90	0.75
$P$ (yr) .....	5.52	$5.53 \pm 0.01$
$M_\eta$ ( $M_\odot$ ) .....	80	70
$M_c$ ( $M_\odot$ ) .....	30	68
$\omega$ (deg) .....		275
$i$ (deg) .....		50
$\gamma$ ( $\text{km s}^{-1}$ ) .....		-12
$\dot{M}_\eta$ ( $M_\odot \text{ yr}^{-1}$ ) .....		$10^{-4}$
$\dot{M}_c$ ( $M_\odot \text{ yr}^{-1}$ ) .....		$10^{-5}$
$V_{\infty,\eta}$ ( $\text{km s}^{-1}$ ) .....		500
$V_{\infty,c}$ ( $\text{km s}^{-1}$ ) .....		2000

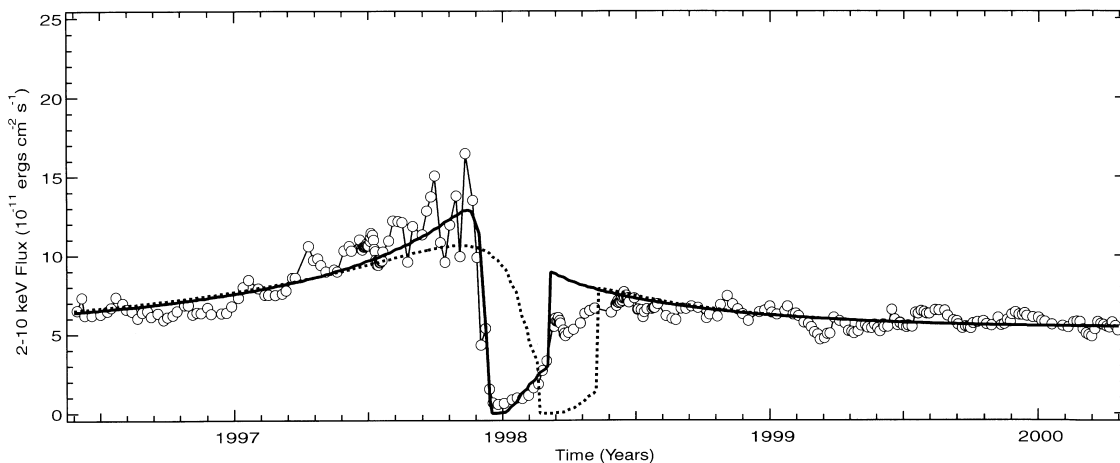


FIG. 3.—*RXTE* light curve of  $\eta$  Carinae and the colliding-wind model (see Table 1), including an interval of enhanced mass loss following periastron passage using the parameters in Table 1, along with an enhanced mass-loss model based on the Damineli et al. (2000) parameters. The extra mass loss from the primary has the effect of suppressing the observed flux from the system for an extended period following periastron passage and provides a better match to the duration of the X-ray eclipse.

based on the Daminieli et al. (2000) values given in Table 1 is shown by the thick dotted line. Our model is an improvement over those published previously (Pittard et al. 1998; Ishibashi et al. 1999), in that the decline to minimum and the asymmetry of the shoulders of the eclipse are better matched (although the model badly fails to match the observed eclipse duration). The ratio of the model flux to the observed X-ray flux determines the distance to  $\eta$  Carinae as  $D \approx 2300$  pc. The formal uncertainty in the distance we derive is primarily influenced by uncertainties in fixing the X-ray flux level outside of the eclipse and is only about 10%. However, uncertainties in the model parameters and other simplifications in the analytic description of the X-ray luminosity may make the real uncertainty in the distance somewhat larger.

The values of  $\dot{M}$  listed in Table 1 are rather uncertain; in particular, we have adopted a rather large value for the mass-loss rate of the companion, i.e.,  $\dot{M}_c = 10^{-5} M_\odot \text{ yr}^{-1}$ , which is more typical of evolved Wolf-Rayet stars than unevolved O-type stars. While the adopted values provide a fairly good match to most of the observed X-ray variability (outside of X-ray minimum), these mass-loss rates are not uniquely defined. Other combinations of  $\dot{M}_\eta$  and  $\dot{M}_c$  can also provide an adequate match to the data, especially if we allow some latitude in choice of terminal velocities. In order to see if any constraints could be placed on mass-loss rates, we ran models with differing values of  $\dot{M}$  for both stars, with the wind terminal velocities and orbital elements held constant at the tabulated values. We found that the mass-loss rate from  $\eta$  Carinae is constrained to be  $\dot{M}_\eta < 3 \times 10^{-4} M_\odot \text{ yr}^{-1}$  in order to match the gradual rise to maximum in the 1997.0–1997.9 interval. Models with  $\dot{M}_\eta$  larger than this limit show significant absorption of the 2–10 keV X-ray emission months prior to periastron, which suppresses the rise in observed flux  $f_x$  up to periastron. In addition, these models generally yield columns of  $N_H > 10^{23} \text{ cm}^{-2}$  at all orbital phases, while the observed columns are typically  $N_H \approx 3 \times 10^{22} \text{ cm}^{-2}$  for most of the orbit (Corcoran et al. 1998, 2000; Ishibashi et al. 1999). As an example of this effect, we include in Figure 2 a model with  $\dot{M}_\eta = 3 \times 10^{-4} M_\odot \text{ yr}^{-1}$ . This model is basically flat through 1997 except for a very brief increase in observed flux very near periastron, in contrast to the observed X-ray variation during this interval. It is more difficult to put constraints on the mass-loss rate from the companion, since the X-ray light curve in the 1996–2000 interval is dominated by the wind from  $\eta$  Carinae. Observations near inferior conjunction/apastron (in 2002.25) may allow us to put tighter constraints on  $\dot{M}_c$  as the companion moves in front of  $\eta$  Carinae.

### 3.2. An Enhanced- $\dot{M}$ Model

While the new orbit model provides an adequate match to the decline to minimum, the width of the eclipse in the model is still much narrower than the observed X-ray eclipse. This is mainly due to the fact that, for any significant orbital eccentricity, the stars move very quickly near periastron, so that the line of sight quickly passes through less dense regions of the wind from  $\eta$  Carinae as the orientation to the colliding-wind shock changes. As noted by Corcoran et al. (2000), however, the anomalously small column density measured by *ASCA* during the X-ray eclipse, and the lack of any enhancement in emission out to 10 keV at that time, may well indicate that the colliding-wind source is completely hidden and that the measured emission is

simply contamination from another source of keV X-rays within the *ASCA* extraction region (i.e., within 3' from  $\eta$  Carinae). *Chandra* imaging at energies above 2 keV does not clearly reveal the presence of any hard source resolved from  $\eta$  Carinae (Seward et al. 2001), which suggests that the source of contamination lies within 0.5' of  $\eta$  Carinae, possibly due to scattering of the colliding-wind flux by dust near the star. Corcoran et al. (2000) noted that a column density  $N_H > 10^{24} \text{ cm}^{-2}$  would be necessary to completely hide the colliding-wind source. A column so large might imply either a nonspherical wind or disk around  $\eta$  Carinae (Ishibashi et al. 1999) or a mass-loss increase near periastron if the wind from  $\eta$  Carinae is spherically symmetric away from the wind-wind collision shock. Because a mass-loss enhancement requires fewer free parameters to model, we adjusted our colliding-wind model to allow for a brief period of enhanced mass loss from  $\eta$  Carinae after periastron. Our best fit is shown as the solid smooth curve in Figure 3. In this model, we assume an increase of a factor of 20 in  $\dot{M}_\eta$  in the interval  $T_0 < t < T_0 + 0.221$  yr; i.e., we assume an interval of mass-loss enhancement by a factor of 20 starting at periastron passage and lasting for about 80 days. The model shown in Figure 3 provides a much better match to the observed duration of the X-ray eclipse. For comparison, we also calculate a similar “enhanced- $\dot{M}_\eta$ ” model with the orbital elements of Daminieli et al. (2000). This model is shown as the broken curve in Figure 3. Figure 4 shows the variation in the model  $N_H$ , relative to the constant- $\dot{M}_\eta$  model.

### 3.3. Expected and Observed Radial Velocities

From their STIS data, Davidson et al. (2000) determined velocity shifts in the range  $-23 \leq \Delta v_{0.7} \leq -4 \text{ km s}^{-1}$  for the Pa 3-7, 3-8, 3-10, and 3-11 emission lines, where  $v_{0.7}$  are the velocities they measured at 70% of the peak of the emission line. The velocities  $v_{0.5}$  at 50% of the emission-line peak lie in the range  $-3 \leq \Delta v_{0.5} \leq +4 \text{ km s}^{-1}$ . The emission-line velocity shifts are much less than the expected shift  $\Delta v \equiv [v(1999.1) - v(1998.2)] = +35 \text{ km s}^{-1}$ , based on the orbital solution of Daminieli et al. (1997, 1999), which Davidson et al. (2000) used for comparison to their STIS data. The orbital solution in Daminieli et al. (2000) implies

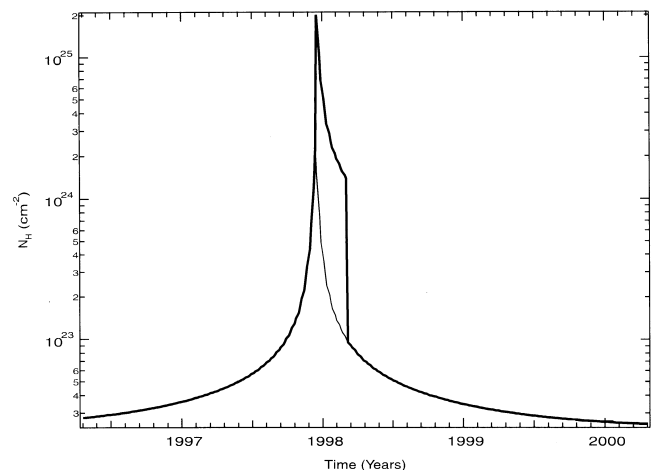


FIG. 4.—Variation in  $N_H$  to the colliding-wind shock. The “enhanced- $\dot{M}_\eta$ ” model is shown by the thick line, and the “constant- $\dot{M}_\eta$ ” model is shown by the thin line. The “enhanced- $\dot{M}_\eta$ ” model provides an extended interval of extra absorption ( $N_H > 10^{24} \text{ cm}^{-2}$ ), which completely hides the colliding-wind shock.

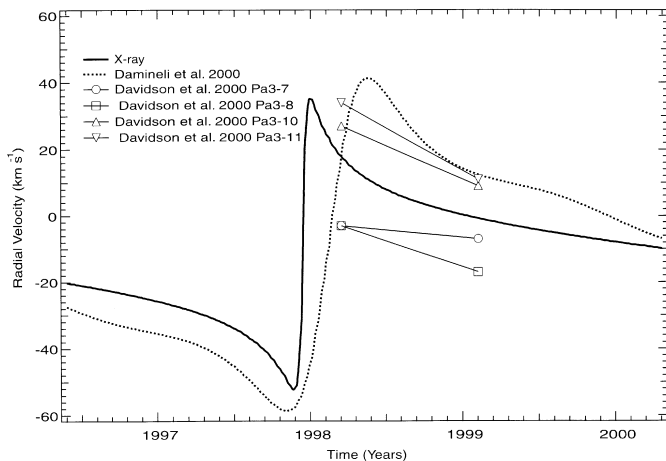


FIG. 5.—The expected radial velocity curve of the primary based on the orbital elements derived in the present work (*solid line*) and on the Damineli et al. (2000) orbital elements (*dotted line*). The  $v_{0.7}$  velocities from the STIS data reported by Davidson et al. (2000) are also shown.

that  $v(1998.2) = +26 \text{ km s}^{-1}$  and  $v(1999.1) = +24 \text{ km s}^{-1}$  or  $\Delta v = -2 \text{ km s}^{-1}$ , in better agreement with some of the STIS observations, though this solution still has serious problems in matching the observed X-ray light curve, as shown in Figures 2 and 3. Figure 5 shows the Damineli et al. (2000) radial velocity curve, and the radial velocity curve based on the “X-ray orbital elements” in Table 1. The symbols show the measured  $v_{0.7}$  velocities from Davidson et al. (2000) for the Paschen lines. Both the Damineli et al. (2000) radial velocity curve and the curve based on the X-ray analysis are bracketed by the measured STIS radial velocities.

#### 4. CONCLUSION

Our attempts to model the *RXTE* light curve of  $\eta$  Carinae strongly suggest the following:

1.  $\eta$  Carinae is a binary star in which the observed properties of the 2–10 keV X-ray emission are primarily due to wind-wind collisions.
2. If the luminosity of the X-ray source varies as the inverse of the separation of the stars, then the duration of the X-ray minimum is very difficult to fit in any colliding-wind model with significant eccentricity and  $i \leq 60^\circ$ , unless the observed flux is artificially suppressed for an interval of time following periastron, possibly due to an enhancement in mass-loss rate at that time.
3. The sharp decline to minimum requires that the last periastron passage occurred at the end of 1997 and not in early 1998.

It might be possible to keep the time of periastron passage as late as 1998.13 if there were a significant mass-loss enhancement prior to periastron passage. Our preliminary exploration of such models suggests that they do not match the observed decline from X-ray maximum to X-ray minimum as well as the model presented here. It is, of course, harder to conjecture physical reasons for an enhancement prior to periastron passage, though full illumination of this point requires detailed modeling of the tidal forces on  $\eta$  Carinae.

In a very eccentric orbit, the increase in tidal force near periastron provides an obvious explanation for an increase in  $\dot{M}_\eta$  at that time, especially if the outer layers of  $\eta$  Carinae

are not tightly bound to the stellar core. The importance of tidally driven mass loss from  $\eta$  Carinae has been previously considered (for example, Davidson 1997). Even if  $e = 0.9$ , the periastron separation is still about  $1.5 \text{ AU} = 320 R_\odot$ , so the stars are not particularly close. However the radius of  $\eta$  Carinae is currently not well constrained and probably lies in the range  $70\text{--}450 R_\odot$  (Davidson 1999), so even in the conservative case, the separation is only about 5 times the stellar radius of  $\eta$  Carinae. It is interesting to speculate that some of the line-profile variability observed near periastron may actually be produced by a combination of a change in radial velocity and a change in circumstellar density.

Along with the phase dependence of  $\dot{M}_\eta$ , another controversial result of our X-ray analysis is the rather low mass-loss rate we derive for  $\eta$  Carinae for most of the orbit. Typical values of  $\dot{M}_\eta$  are generally  $\sim 10^{-3} M_\odot \text{ yr}^{-1}$ , not  $\sim 10^{-4} M_\odot \text{ yr}^{-1}$ , which we claim as the true mass-loss rate for  $\eta$  Carinae for most of the 5.52 year cycle. However, the mass-loss rate from  $\eta$  Carinae is not well constrained by observations in other regions of the EM spectrum. Andriessse, Donn, & Viotti (1978) derived a value of  $\dot{M}_\eta \approx 7.5 \times 10^{-2} M_\odot \text{ yr}^{-1}$  based on their analysis of the dust formation rate, while van Genderen & The (1984) estimated that  $\dot{M}_\eta \approx 10^{-4} M_\odot \text{ yr}^{-1}$  based on a number of arguments. Davidson (1987) gave  $\dot{M}_\eta < 10^{-3} M_\odot \text{ yr}^{-1}$ . Radio observations (White et al. 1994) near the X-ray minimum in 1992 yielded  $\dot{M}_\eta \approx 3 \times 10^{-4} M_\odot \text{ yr}^{-1}$ . An STIS spectrum obtained in 1998 March (coincidentally near the time of our “enhanced mass loss” interval) and analyzed by Hillier et al. (2000) yielded a value of  $\dot{M}_\eta \approx 10^{-3} M_\odot \text{ yr}^{-1}$ . Millimeter observations (Cox et al. 1995; Cox 1997) yielded values of  $\dot{M}_\eta \approx 10^{-3} M_\odot \text{ yr}^{-1}$ . We should point out that most of these other mass-loss rate estimates have assumed that  $\eta$  Carinae is a single star. This assumption neglects the effect of the companion on the ionization balance in the outer wind of  $\eta$  Carinae, which in turn can significantly affect mass-loss estimates based on emission-line profiles or the amount of free-free emission. Since the X-ray absorption is primarily produced by K-shell absorption, the derived X-ray mass-loss rates are not greatly affected by the wind ionization, as long as the wind is not fully ionized.

While we have modeled the X-ray eclipse as an interval of enhanced X-ray absorption, an alternative possibility is that the long X-ray minimum might represent a reduction of the intrinsic X-ray emission. Such a reduction presumably could be produced if the winds near periastron collide at velocities much less than their terminal speeds. The relative collision velocities could be less near periastron if the winds from one or both stars have slower accelerations than winds from other massive stars or if radiative braking (Gayley, Owocki, & Cranmer 1997) is important. The duration of the X-ray eclipse in the model could be extended without an enhancement in  $\dot{M}_\eta$  if the inclination is closer to  $90^\circ$ , since then the line of sight to the X-ray source passes through very dense regions of the wind from  $\eta$  Carinae for an extended period near conjunction. However, large values of inclination seem ruled out by lack of phase-dependent optical variability. It is worth noting that, for values of  $i \sim 50^\circ$ , and if the wind eclipse is complete, then conjunction must occur near periastron since, otherwise, there is not enough wind material along the line of sight to produce much absorption at energies above 5 keV.

We expect that STIS (or other high spatial resolution) Paschen-line observations of the core of  $\eta$  Carinae near the

next periastron passage (2003.5) will show large velocity shifts if the binary model presented here is correct and the mass ratio is not too extreme. However, if significant variations in the ionization, the density, and/or emitting volume near periastron passage occur, then determining accurate radial velocities and orbital elements from the emission lines may be difficult even with STIS. The X-ray fluxes, however, should be relatively insensitive to these effects. We point out that the variable P Cygni absorption components seen in the STIS data (Hillier et al. 2000) may provide a better estimate of the orbit than either the STIS emission lines or the X-ray fluxes, since for the absorption components, the absorbing volume is constrained to lie in front of the stellar disk. Coordinated X-ray and STIS spectral

observations of the P Cygni lines near periastron will be especially useful to fully constrain the orbit.

We thank Frank Chung, a student intern from Eleanor Roosevelt High School, Greenbelt, MD, for his assistance in generating model fits to the *RXTE* light curve. We also thank Stan Owocki, Kris Davidson, and the referee, David Cohen, for enlightening comments which have significantly improved this paper. This work made use of the FTOOLS suite of software supported by the HEASARC. The *RXTE* observations were supported by NASA grant NAS 5-32490. This research has made use of NASA's Astrophysics Data System Abstract Service.

## REFERENCES

- Andriess, C. D., Donn, B. D., & Viotti, R. 1978, *MNRAS*, 185, 771  
 Bradt, H. V., Rothschild, R. E., & Swank, J. H. 1993, *A&AS*, 97, 355  
 Corcoran, M. F., Ishibashi, K., Davidson, K., Swank, J. H., Petre, R., & Schmitt, J. H. M. M. 1997, *Nature*, 390, 587  
 Corcoran, M. F., et al. 1998, *ApJ*, 494, 381  
 ———. 2000, *ApJ*, in press  
 Corcoran, M. F., Rawley, G. L., Swank, J. H., & Petre, R. E. 1995, *ApJ*, 445, L121  
 Cox, P. 1997, in *ASP. Conf. Ser. 120, Luminous Blue Variables: Massive Stars in Transition*, ed. A. Nota & H. J. G. L. M. Lamers (San Francisco: ASP), 277  
 Cox, P., et al. 1995, *A&A*, 297, 168  
 Damineli, A. 1996, *ApJ*, 460, L49  
 Damineli, A., Conti, P. S., & Lopes, D. F. 1997, *NewA*, 2, 107  
 Damineli, A., Kaufer, A., Wolf, B., Stahl, O., Lopes, D. F., & Araújo, F. X. 2000, *ApJ*, 528, L101  
 Damineli, A., Lopes, D. F., & Conti, P. S. 1999, in *ASP. Conf. Ser. 179,  $\eta$  Carinae at the Millennium*, ed. J. A. Morse, R. M. Humphreys, & A. Damineli (San Francisco: ASP), 288  
 Davidson, K. 1987, *ApJ*, 317, 760  
 Davidson, K. 1997, *NewA*, 2, 387  
 ———. 1999, in *ASP. Conf. Ser. 179,  $\eta$  Carinae at the Millennium*, ed. J. A. Morse, R. M. Humphreys, & A. Damineli (San Francisco: ASP), 6  
 Davidson, K., Ishibashi, K., Gull, T. R., Humphreys, R. M., & Smith, N. 2000, *ApJ*, 530, L107  
 Duncan, R. A., et al. 1995, *ApJ*, 441, L73  
 Gayley, K., Owocki, S. P., & Cranmer, S. 1997, *ApJ*, 475, 786  
 Hillier, D. J., Davidson, K., Ishibashi, K., & Gull, T. 2000, *ApJ*, in press  
 Ishibashi, K. 1999, Ph.D. thesis, Univ. Minnesota  
 Ishibashi, K., Corcoran, M. F., Davidson, K., Swank, J. H., Petre, R., Drake, S. A., Damineli, A., & White, S. 1999, *ApJ*, 524, 983  
 Pittard, J. M., Stevens, I. R., Corcoran, M. F., & Ishibashi, K. 1998, *MNRAS*, 299, L5  
 Seward, F. D., et al. 2001, *ApJ*, submitted  
 Tanaka, Y., Inoue, H., & Holt, S. S. 1994, *PASJ*, 46, L37  
 Usov, V. V. 1992, *ApJ*, 389, 635  
 Vanbeveren, V., De Loore, C., & Van Rensbergen, W. 1998, *A&A Rev.*, 9, 63  
 van Genderen, A. M., & The, P. S. 1984, *Space Sci. Rev.*, 39, 317  
 White, S. M., et al. 1994, *ApJ*, 429, 380